Investigation of polar stratospheric cloud solid particle formation mechanisms using ILAS and AVHRR observations in the Arctic

H. Irie,[1] K. L. Pagan,[2,3] A. Tabazadeh,[4] M. J. Legg,[5,3] and T. Sugita[6]

Received 14 April 2004; revised 30 June 2004; accepted 13 July 2004; published 10 August 2004.

[1] Satellite observations of denitrification and ice clouds in the Arctic lower stratosphere in February 1997 are used with Lagrangian microphysical box model calculations to evaluate nucleation mechanisms of solid polar stratospheric cloud (PSC) particles. The occurrences of ice clouds are not correlated in time and space with the locations of back trajectories of denitrified air masses, indicating that ice particle surfaces are not always a prerequisite for the formation of solid PSCs that lead to denitrification. In contrast, the model calculations incorporating a pseudo-heterogeneous freezing process occurring at the vapor-liquid interface can quantitatively explain most of the observed denitrification when the nucleation activation free energy for nitric acid dihydrate formation is raised by only ~10% relative to the current published values. Once nucleated, the conversion of nitric acid dihydrate to the stable trihydrate phase brings the computed levels of denitrification closer to the measurements. *INDEX TERMS:* 0305 Atmospheric Composition and Structure: Aerosols and particles (0345, 4801); 0320 Atmospheric Composition and Structure: Cloud physics and chemistry; 0340 Atmospheric Composition and Structure: Middle atmosphere—composition and chemistry. **Citation:** Irie, H., K. L. Pagan, A. Tabazadeh, M. J. Legg, and T. Sugita (2004), Investigation of polar stratospheric cloud solid particle formation mechanisms using ILAS and AVHRR observations in the Arctic, *Geophys. Res. Lett.*, *31*, L15107, doi:10.1029/2004GL020246.

1. Introduction

[2] It has been well established that large, nitric acid (HNO_3)-containing polar stratospheric cloud (PSC) particles (>5 μm in size), which are shown to cause denitrification in the Arctic, are most likely composed of nitric acid trihydrate (NAT) [*Fahey et al.*, 2001], although nitric acid dihydrate (NAD) cannot be ruled out as a possible composition [e.g., *Tabazadeh et al.*, 2001; *Carslaw et al.*, 2002]. In order for solid HNO_3 PSCs to grow to such large sizes, a selective nucleation process must be involved. Previously, *Irie and Kondo* [2003] used nucleation rates reported by *Salcedo et al.* [2001] in a microphysical model to show that homogeneous nucleation of NAD and NAT in liquid ternary ($H_2SO_4/HNO_3/H_2O$) aerosols (LTAs) can explain the observed Arctic denitrification in February 1997. However, *Knopf et al.* [2002] have recently argued that the reported homogeneous freezing rates of *Salcedo et al.* [2001] for concentrated solutions of aqueous HNO_3 cannot be linearly extrapolated to more dilute systems, which are representative of the lower stratosphere. Although the arguments put forward by *Knopf et al.* [2002] are valid for homogeneous freezing, stratospheric droplets may still freeze pseudo-heterogeneously at the vapor-liquid interface [*Tabazadeh et al.*, 2002].

[3] In this paper, we use measurement/model comparisons to investigate two possible nucleation processes, namely nucleation of NAT on preexisting ice particle surfaces [*Wofsy et al.*, 1990; *Carslaw et al.*, 2002] and pseudo-heterogeneous surface freezing of NAD particles from LTA solutions [*Tabazadeh et al.*, 2002]. For the set of measurements discussed in this work, we show that ice particle surfaces could not have caused the nucleation of nitric acid hydrate particles that cause denitrification. We also investigate under what set of assumptions a surface nucleation mechanism can explain the Arctic denitrification observed.

2. ILAS and AVHRR Observations

[4] The Improved Limb Atmospheric Spectrometer (ILAS) onboard the Advanced Earth Observing Satellite (ADEOS) uses a solar occultation technique to measure vertical profiles of HNO_3 and nitrous oxide (N_2O) concentrations and aerosol extinction coefficient (AEC) at 780 nm with a vertical resolution of ~2 km in the Arctic vortex. The present study uses version 5.2 ILAS data. Using HNO_3-N_2O correlations obtained under PSC-free conditions (based on AEC data), the permanent loss of HNO_3 by denitrification was quantified as the difference between the measured HNO_3 values and those given from the tight HNO_3-N_2O correlation obtained in early February just prior to denitrification (see *Kondo et al.* [2000], *Irie et al.* [2001], and *Irie and Kondo* [2003] for more details). We focus on air masses observed under PSC-free conditions at 19–20 km inside the Arctic vortex in January–February 1997. At these altitudes, the uncertainties in estimating HNO_3 losses, defined as 3-σ standard deviations, are as small as 2 ppbv, almost independent of the error in the N_2O data.

[5] In the 1996/1997 winter, the Advanced Very High Resolution Radiometer (AVHRR) onboard the National Oceanic and Atmospheric Administration (NOAA) 12 and 14 satellites measured thermal infrared emissions at 10.9 and 11.9 μm (channels 4 and 5, respectively). We derived ice PSC regions from the AVHRR channel 5 brightness temperature (T_5) and the channel 4–5 brightness temperature difference (BTD) using an ice PSC detection algorithm [*Hervig et al.*, 2001; *Pagan et al.*, 2004]. Although ice PSCs and cirrus clouds are both high, cold ice clouds, ice PSCs are generally colder and have lower optical depths and

[1]Frontier Research System for Global Change, Yokohama, Japan.
[2]San Francisco State University, San Francisco, California, USA.
[3]Now at NASA Ames Research Center, Moffett Field, California, USA.
[4]NASA Ames Research Center, Moffett Field, California, USA.
[5]Bay Area Environmental Research Institute, Sonoma, California, USA.
[6]National Institute for Environmental Studies, Tsukuba, Ibaraki, Japan.

0094-8276/04/2004GL020246$05.00

smaller particle sizes than cirrus clouds, resulting in a colder T_5 and a larger BTD for ice PSCs. These differences allow us to identify ice PSCs by comparing measured T_5 and BTD values from thermal infrared imagery on a pixel-by-pixel basis with those for a modeled cirrus layer located at the tropopause. The ice PSC detection algorithm is a 2-step process. The first step maps optically thick PSCs by identifying pixels with AVHRR T_5 colder than the tropopause temperature and AVHRR BTD larger than 2.0. The second step maps optically thin ice PSCs by identifying pixels where the AVHRR BTD exceeds the maximum BTD for the modeled cirrus layer. Since BTDs for ice PSCs and cirrus can overlap, we also use the regions where the "mean modeled cirrus BTD" < AVHRR BTD < "maximum modeled cirrus BTD," which are referred to as "probable ice PSCs." The regions with AVHRR BTDs below the mean modeled cirrus BTD are excluded, because they are most likely cirrus, other tropospheric clouds, or land features. Using this algorithm, we produced daily ice PSC maps with a spatial resolution of 4 km × 4 km for the Arctic region in February 1997.

3. Lagrangian Microphysical Box Model

[6] We used a Lagrangian microphysical box model (including nucleation, growth, and sedimentation) [*Larsen*, 2000; *Irie and Kondo*, 2003] to calculate the temporal changes in HNO_3 along twenty-day isentropic back trajectories for the air masses observed by ILAS under PSC-free conditions inside the Arctic vortex in January–February 1997. Trajectories were calculated using European Centre for Medium-Range Weather Forecasts (ECMWF) data and codes of *Matsuzono et al.* [1998]. The temperatures along the trajectories were adjusted downward assuming a 1-K bias in ECMWF temperatures [*Knudsen*, 1996]. Vortex air masses at 19–20 km experienced diabatic descent of ~15 K (~1 km) over 20 days [*Knudsen et al.*, 1998]. We did not consider this effect in trajectory calculations because the mean vertical gradients of temperature and HNO_3 at 19–20 km inside the vortex were as small as −0.2 K/km and −0.2 ppbv/km, respectively. The microphysical model uses a scheme for the nucleation of NAD on the surfaces of LTA droplets [*Tabazadeh et al.*, 2002]. HNO_3 and H_2O mixing ratios were initialized using ILAS data obtained inside the Arctic vortex in early February 1997 before the onset of denitrification [*Irie et al.*, 2001]. A non-volcanic value of 0.3 ppbv was used for H_2SO_4 mixing ratio [*Irie and Kondo*, 2003]. In February 1997, significant denitrification occurred at altitudes up to 21 km in the Arctic [*Irie et al.*, 2001]. Considering that denitrification occurs in all of the layers where particles fall taking up gas-phase HNO_3, denitrification observed by ILAS at 19–20 km could be caused by the particles nucleated at altitudes up to 21 km. To take this possible sedimentation into account, additional model calculations were performed at 21 km. Temperatures at 21 km were derived from trajectory temperatures using the mean vertical temperature gradient given by ECMWF data in February 1997. Since the twenty-day trajectory calculations may introduce uncertainties into the microphysical modeling, sensitivity tests were performed with the trajectory temperatures varied over ±1 K and with initial HNO_3 values varied over ±2 ppbv. For these ranges, the model is more sensitive to HNO_3 than temperature, so that calculations performed only for the HNO_3 uncertainty are discussed below. In the present study, two sets of model calculations were performed assuming that (1) denitrification was caused by sedimentation of NAD particles and (2) denitrification was caused by sedimentation of NAT particles, which were produced via an instantaneous conversion from NAD nuclei [e.g., *Worsnop et al.*, 1993].

4. Nucleation on Ice Particle Surfaces

[7] At 19–20 km in February 1997, ILAS observed 21 air masses with significant denitrification (more than 2 ppbv loss in HNO_3) over the Arctic. Daily locations of back trajectories for these air masses were compared with corresponding daily ice PSC maps produced from AVHRR data to identify the air masses that had traversed the ice PSC regions. The method of analysis described here for the ILAS data is similar to that described by *Pagan et al.* [2004]. The results from the *Pagan et al.* [2004] study revealed that lidar observations of solid HNO_3 particles in early December 1999 were not correlated in time and space with locations of ice cloudiness in the Arctic stratosphere. Similarly, below we show a lack of correlation between areas where denitrification was seen by ILAS and the areas of ice cloudiness in the Arctic.

[8] Here, we identified ice PSC-influenced air masses when the distance between the trajectory and the ice PSCs was less than 100 km on the same day. To consider the errors in the trajectory calculations, a 300-km distance threshold was also used as the influence criterion, although further errors may affect the results. Since AVHRR is a nadir-viewing instrument, it is very difficult to determine the exact altitudes at which the ice PSCs observed were generated. Because of this limitation, we assumed that all the ice PSCs observed by AVHRR were at the same altitude or within a few kilometers above the trajectories. In addition, the regions identified as "probable ice PSCs" and ice PSC patches as small as 4 km × 4 km were also included in the ice PSC regions. These procedures likely yield an upper limit for the number of air masses traversing the ice PSC regions.

[9] Using the 100-km threshold and considering all 21 denitrified air masses, only 5 air masses were judged to have traversed the ice PSC regions in February. Using the 300-km threshold yielded only 12 of the 21 air masses as having traversed the ice PSC regions. An example of our analyses, the ice PSC map and back trajectories for one day, February 10, 1997, is shown in Figure 1. A region of ice PSCs and probable ice PSCs is shown over the northern coast of Greenland. The three back trajectories (solid, dashed, and dotted lines) show the location of the denitrified air masses on February 10. These trajectories were not within 100 km of the ice PSCs; rather, they were within 300 km. Of the 21 ILAS air masses that showed significant denitrification, 9 (or about 43%) air mass trajectories showed no correlation with the ice PSC regions observed by AVHRR. This lack of correlation is further supported by the fact that the mean magnitude (±standard deviation) of denitrification for the 12 air masses that had traversed the ice PSC regions (4.2 ± 1.6 ppbv) was almost equal to that for other air masses (4.7 ± 1.0 ppbv). Overall, the analyses presented above combined with the study of *Pagan et al.* [2004] suggest that ice particle surfaces are not always a

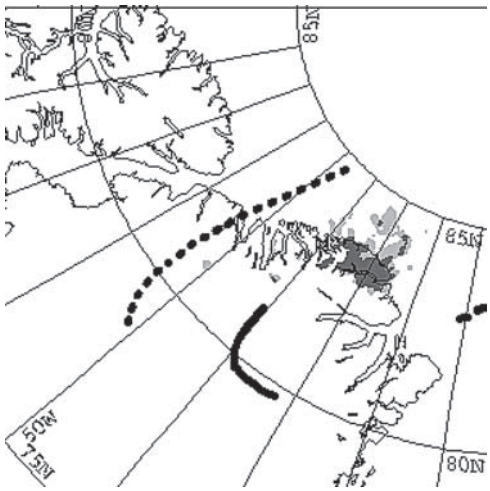

Figure 1. AVHRR-detected ice PSC regions (dark gray) over the northern coast of Greenland for February 10, 1997. The regions categorized as "probable ice PSCs" (light gray) are also shown. Three back trajectories, showing only portions for February 10, are for denitrified air masses observed by ILAS at 19–20 km at 69°N and 61°W on February 17 (solid line), 69°N and 87°W on February 17 (dashed line), and 69°N and 54°W on February 18 (dotted line).

prerequisite for the formation of nitric acid hydrate PSCs that lead to denitrification.

5. Nucleation on LTA Droplet Surfaces

[10] We next compare losses of HNO_3 by denitrification observed by ILAS with those calculated by the microphysical box model to investigate a possible role of nucleation of NAD on LTA droplet surfaces in denitrification. In this model, the production rate (P) of NAD nuclei (cm^{-3} s^{-1}) is given by:

$$P = JS$$

$$J = N(kT/h)\exp\left(\frac{-\Delta G}{RT}\right),$$

where J (cm^{-2} s^{-1}) is the number of NAD nuclei formed per second on a unit surface area of the liquid, S (cm^2 cm^{-3}) is the total surface area of all droplets per unit volume of air, N (cm^{-2}) is the total number of molecules per unit surface area of the liquid (N is calculated by multiplying the HNO_3 mole fraction (X_{HNO_3}) in the solution by the approximate molecular site density of 10^{15} cm^{-2}), k (J K^{-1}) is the Boltzmann constant, h (J s) is the Planck constant, T (K) is temperature, and R (kcal mol^{-1} K^{-1}) is the ideal gas constant. According to *Tabazadeh et al.* [2002], the free energy of NAD nucleus formation on the LTA surfaces (ΔG) in kcal mol^{-1} is given by:

$$\Delta G = 11.5593 + 0.0804214T - (71.5133 - 0.256724)X_{HNO_3}$$

[11] Because of limited laboratory data, the above expression is valid for $0.246 < X_{HNO_3} < 0.333$ [*Salcedo et al.*, 2001; *Tabazadeh et al.*, 2002]. Extrapolation of the above relation to stratospheric conditions may introduce additional uncertainty in ΔG since X_{HNO_3} in stratospheric LTAs is typically smaller than 0.18. For example, ΔG changes of ±10% (corresponding to ~2.3 kcal mol^{-1} at $X_{HNO_3} = 0.18$ and $T = 190$ K) alter P values by over three orders of magnitude. Thus, the estimate of ΔG for the stratosphere is critical to simulate denitrification. Below, we performed model calculations to constrain ΔG values in the model in order to maximize the agreement between the modeled and observed levels of denitrification.

[12] Figure 2a shows comparisons of losses in HNO_3 by denitrification observed by ILAS with those calculated by the model, using ΔG of the above expressions. This model assumes that denitrification was caused by growth and sedimentation of NAD. As seen in the figure, the magnitudes of denitrification from the model did not tightly correlate with the ILAS observations ($R^2 = 0.24$). We then performed sensitivity studies to match the observations by changing ΔG in the model. We found the best agreement ($R^2 = 0.60$) when the ΔG values were increased by only 9.5% compared to values from the above reported expressions (Figure 2b). The model calculations with initial HNO_3 values varying over ±2 ppbv are shown with error bars only for observed denitrification of 2–7 ppbv. We note here that significant differences exist between the model calculations and ILAS observations for air masses where the observed levels of denitrification were in the range of 2 to 4 ppbv (Figure 2b). To search for the cause of this discrepancy, we performed additional model calculations, allowing instantaneous conversion of NAD nuclei into NAT (i.e., sedimentation of NAT) (Figures 3a and 3b). As seen in

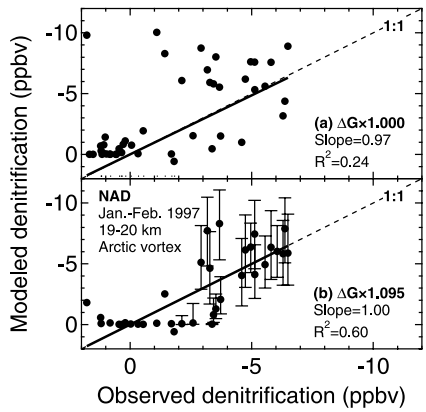

Figure 2. Comparisons of magnitudes of denitrification from the model and ILAS observations for the data obtained inside the Arctic vortex in January–February 1997. The data with model values ranging between −0.01 and 0.01 ppbv are excluded for clarity. The calculation was made using a microphysical box model assuming that NAD particles nucleated, grew, and fell to lower altitudes. (a) Original ΔG values obtained by *Tabazadeh et al.* [2002] and (b) adjusted values (×1.095) were used for the calculation of NAD nucleation rates. The thick solid lines represent the linear least-squares fits to the data. The model calculations with initial HNO_3 values varying over ±2 ppbv are shown with error bars only for observed denitrification of 2–7 ppbv.

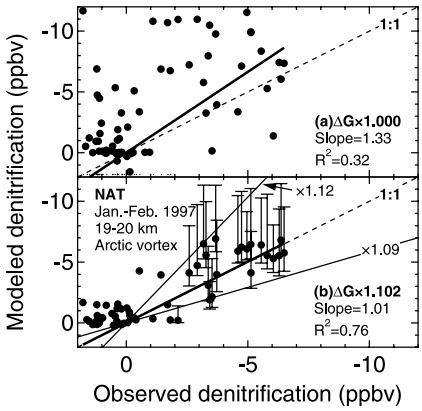

Figure 3. Same as Figure 2 except that the model calculation was made assuming that NAT particles converted from NAD nuclei grew and fell to lower altitudes. (a) Original ΔG values and (b) adjusted values ($\times 1.102$) were used for the calculation of NAD nucleation rates. Data enclosed by two thin lines can be explained by the model when ΔG values are raised by 9–12%.

Figure 3b, where ΔG values were increased by only 10.2%, the agreement for the observed denitrification in the range of 2 to 4 ppbv was improved when NAD was instantaneously converted to NAT in the model.

[13] In general, we could account for the observed denitrification in most air masses when ΔG values used in the model were raised by only 9 to 12% (Figure 3b) as compared to the original reported values [*Tabazadeh et al.*, 2002]. Since the original ΔG values were based on laboratory data obtained for concentrated solutions of HNO_3 [*Salcedo et al.*, 2001], we find a change of $\sim$10% for more dilute stratospheric solutions to be a reasonable adjustment. However, since this adjustment may be somewhat uncertain, laboratory data under relevant stratospheric conditions are highly desirable to obtain quantitative rate expressions for this possible nucleation freezing process.

6. Conclusions

[14] We used ILAS HNO_3, N_2O, H_2O, and AEC measurements, AVHRR stratospheric ice cloud measurements, and a microphysical box model to investigate processes leading to denitrification in the Arctic vortex in February 1997. Back trajectory analyses showed that about 40% of the denitrified air masses observed by ILAS did not pass through ice cloud regions, ruling out the possible role of ice clouds in causing the observed denitrification. Microphysical box model calculations, including a pseudo-heterogeneous freezing mechanism, could explain the observed levels of denitrification when NAD freezing energy was increased by $\sim$10% as compared to current values reported in the literature. The agreement in the magnitudes of denitrification between ILAS and the model was improved when NAD was allowed to instantaneously convert to NAT. Finally, our results suggest that sedimentation of NAD or NAT particles formed through NAD freezing on LTA surfaces can cause significant denitrification in the Arctic vortex.

[15] **Acknowledgments.** We appreciate the contributions of all members of the ILAS science team. The AVHRR data were obtained through the NOAA satellite active archive.

References

Carslaw, K. S., J. A. Kettleborough, M. J. Northway, S. Davies, R. S. Gao, D. W. Fahey, D. G. Baumgardner, M. P. Chipperfield, and A. Kleinböhl (2002), A vortex-scale simulation of the growth and sedimentation of large nitric acid hydrate particles, *J. Geophys. Res.*, *107*(D20), 8300, doi:10.1029/2001JD000467.

Fahey, D. W., et al. (2001), The detection of large HNO_3-containing particles in the winter Arctic stratosphere, *Science*, *291*, 1026–1031.

Hervig, M. E., K. L. Pagan, and P. G. Foschi (2001), Analysis of polar stratospheric cloud measurements from AVHRR, *J. Geophys. Res.*, *106*, 10,363–10,374.

Irie, H., and Y. Kondo (2003), Evidence for the nucleation of polar stratospheric clouds inside liquid particles, *Geophys. Res. Lett.*, *30*(4), 1189, doi:10.1029/2002GL016493.

Irie, H., M. Koike, Y. Kondo, G. E. Bodeker, M. Y. Danilin, and Y. Sasano (2001), Redistribution of nitric acid in the Arctic lower stratosphere during the winter of 1996–1997, *J. Geophys. Res.*, *106*(D19), 23,139–23,150.

Knopf, D. A., T. Koop, B. P. Luo, U. G. Weers, and T. Peter (2002), Homogeneous nucleation of NAD and NAT in liquid stratospheric aerosols: Insufficient to explain denitrification, *Atmos. Chem. Phys.*, *2*, 207–214.

Knudsen, B. M. (1996), Accuracy of arctic stratospheric temperature analyses and the implications for the prediction of polar stratospheric clouds, *Geophys. Res. Lett.*, *23*, 3747–3750.

Knudsen, B. M., et al. (1998), Ozone depletion in and below the Arctic vortex for 1997, *Geophys. Res. Lett.*, *25*, 627–630.

Kondo, Y., H. Irie, M. Koike, and G. E. Bodeker (2000), Denitrification and nitrification in the Arctic stratosphere during the winter of 1996–1997, *Geophys. Res. Lett.*, *27*, 337–340.

Larsen, N. (2000), Polar stratospheric clouds, microphysical and optical models, *Sci. Rep. 00-06*, Dan. Meteorol. Inst., Copenhagen.

Matsuzono, T., T. Sano, and T. Ogawa (1998), Development of the trajectory analysis model (EORC/TAM), technical report, Earth Obs. Res. Cent., Tokyo.

Pagan, K. L., A. Tabazadeh, K. Drdla, M. E. Hervig, S. D. Eckermann, E. V. Browell, M. J. Legg, and P. G. Foschi (2004), Observational evidence against mountain-wave generation of ice nuclei as a prerequisite for the formation of three solid nitric acid polar stratospheric clouds observed in the Arctic in early December 1999, *J. Geophys. Res.*, *109*, D04312, doi:10.1029/2003JD003846.

Salcedo, D., L. T. Molina, and M. J. Molina (2001), Homogeneous freezing of concentrated aqueous nitric acid solutions at polar stratospheric temperatures, *J. Phys. Chem. A*, *105*, 1433–1439.

Tabazadeh, A., E. J. Jensen, O. B. Toon, K. Drdla, and M. R. Schoeberl (2001), Role of the stratospheric polar freezing belt in denitrification, *Science*, *291*, 2591–2594.

Tabazadeh, A., Y. S. Djikaev, P. Hamill, and H. Reiss (2002), Laboratory evidence for surface nucleation of solid polar stratospheric cloud particles, *J. Phys. Chem. A*, *106*, 10,238–10,246.

Wofsy, S. C., R. J. Salawitch, J. H. Yatteau, M. B. McElroy, B. W. Gandrud, J. E. Dye, and D. Baumgardner (1990), Condensation of HNO_3 on falling ice particles: Mechanism for denitrification of the polar stratosphere, *Geophys. Res. Lett.*, *17*(4), 449–452.

Worsnop, D. R., L. E. Fox, M. S. Zahniser, and S. C. Wofsy (1993), Vapor pressures of solid hydrates of nitric acid: Implications for polar stratospheric clouds, *Science*, *259*, 71–74.

H. Irie, Frontier Research System for Global Change, 3173-25 Showa-machi, Kanazawa-ku, Yokohama, Kanagawa, 236-0001, Japan. (irie@jamstec.go.jp)

M. J. Legg and K. L. Pagan, NASA Ames Research Center, MS 245-5, Moffett Field, CA 94035-1000, USA.

T. Sugita, National Institute for Environmental Studies, 16-2, Onogawa, Tsukuba, Ibaraki 305-8506, Japan.

A. Tabazadeh, NASA Ames Research Center, MS 245-4, Moffett Field, CA 94035-1000, USA.